Chemical Engineering Journal 97 (2004) 27–35

Chemical Engineering Journal

www.elsevier.com/locate/cej

Modeling of fluidized bed reactor of ethylene polymerization

Mahmood Alizadeh [a], Navid Mostoufi [a,*], Saeed Pourmahdian [b], Rahmat Sotudeh-Gharebagh [a]

[a] *Department of Chemical Engineering, Faculty of Engineering, Process Design and Simulation Research Center, University of Tehran, P.O. Box 11365/4563, Tehran, Iran*

[b] *Department of Polymer Engineering, Amirkabir University of Technology, Tehran, Iran*

Received 7 January 2003; accepted 5 May 2003

Abstract

A pseudo-homogeneous model is proposed for describing the behavior of fluidized bed reactor for linear low density polyethylene (LLDPE) production. The kinetic model employed in this study is based on the moment equations. The average concentration of particles in the bed is estimated from the dynamic two-phase structure hydrodynamic model. A tanks-in-series model was adopted to describe the flow pattern in the reactor. The hydrodynamic and kinetic models are integrated to the reactor model to make a comprehensive gas-phase LLDPE production reactor model. It has been shown that the results of this model fit the actual data in terms of melt flow index of the produced polyethylene, satisfactorily. The proposed model is capable of predicting the performance of the reactor as well as polymer physico-chemical properties.

Keywords: Fluidized bed; Polyethylene polymerization; Ziegler–Natta; Reactor modeling; Moment equations

1. Introduction

Fluidized bed reactors have found broad applications in many chemical processes involving gas–solid and solid-catalyzed gas-phase reactions. Production of linear low density polyethylene (LLDPE) through heterogeneous Ziegler–Natta catalysts is an example of such industrial applications of fluidized beds. Due to operation at lower pressures and temperatures, no need to solvent and better heat removal, compared to the other polyethylene production processes, gas-phase polymerization of ethylene in fluidized bed is now widely employed at industrial scale [1].

Modeling of LLDPE production in fluidized bed reactors has recently received considerable attention. Several research efforts have been conducted on modeling of the fluidized bed reactors for LLDPE production and particle growth models in the reactor [2–6]. These attempts have led to a more realistic understanding of the reactor behavior as well as the properties of the polymer produced in the reactor. Ray [7] considered a modeling hierarchy as microscale, mesoscale and macroscale, based on the characteristics of the polymerization reactor systems. In such approach, overall mass and energy balance and heat removal from the reactor is considered in macroscale level. Particle growth, intraparticle and interparticle mass and energy balance occur at the mesoscale level, while the kinetics of polymerization corresponds to microscale level. Therefore, in order to model such a reactor, phenomena such as complex flow characteristics of gas and solids, kinetics of heterogeneous polymerization, and various heat and mass transfer mechanisms have to be incorporated in a realistic manner [2].

Fluidized bed reactors were modeled as single-, two- or three-phase reactors. In case of LLDPE production in fluidized bed reactors, models such as single-phase continuous stirred tank reactor (CSTR) [4], two-phase [2], and heterogeneous three-phase plug flow reactor (PFR) for all phases [6] have been used. Wu and Baeyens [8] introduced a mixing index, ranging from 0 to 1, for quantifying the extent of mixing in fluidized bed reactors. For a typical ethylene polymerization reactor, the mixing index was estimated to be about 0.4–0.5 which could be interpreted as a poor mixing [6]. This indicates that the fluidized bed reactor of LLDPE production does not behave either as a CSTR or a PFR but its hydrodynamics is situated between these two ideal cases. Therefore, a tanks-in-series model may be used for such a non-ideal reactor which behaves between PFR and CSTR [9].

For young polymer particles containing highly active catalysts, heat and mass transfer resistances may become significant, leading to multiple steady states and particle overheating [4]. The activity of Ziegler–Natta catalyst is

* Corresponding author. Tel.: +98-21-611-2865; fax: +98-21-695-7784.
E-mail address: mostoufi@ut.ac.ir (N. Mostoufi).

1385-8947/$ – see front matter © 2003 Elsevier B.V. All rights reserved.
doi:10.1016/S1385-8947(03)00133-5

Nomenclature

A	cross-section area of the reactor (m^2)
$AlEt_3$	triethyl aluminum
C_A	concentration of component A in the feed gas (kmol/m^3)
C_{A_0}	inlet concentration of component A (kmol/m^3)
C_{A_i}	concentration of component A in CSTR number i (kmol/m^3)
d_p	particle diameter (m)
D_t	reactor inside diameter (m)
j	active site type number
k_{ds}	spontaneous deactivation rate constant (s^{-1})
k_{fh_i}	transfer to hydrogen rate constant for a polymer chain with terminal monomer i (m^3/kmol s)
$k_{fm_{ik}}$	transfer to monomer k rate constant for a polymer chain with terminal monomer i (m^3/kmol s)
k_{fr_i}	transfer to cocatalyst rate constant for a polymer chain with terminal monomer i (m^3/kmol s)
k_{fs_i}	spontaneous transfer rate constant for a polymer chain with terminal monomer i (m^3/kmol s)
k_{h_i}	rate constant for reinitiation by monomer i (m^3/kmol s)
k_{h_r}	rate constant for reinitiation by cocatalyst i (m^3/kmol s)
k_{i_i}	rate constant for initiation by monomer i (m^3/kmol s)
$k_{p_{ik}}$	propagation rate constant for a polymer chain with terminal monomer i reacting with monomer k (m^3/kmol s)
H	height of the reactor (m)
m	number of types of monomers
M_i	monomer of type i
M_n	number average molecular weight (kg/kmol)
M_w	weight average molecular weight (kg/kmol)
MFI	melt flow index of polymer (g per 10 min)
mw	molecular weight (kg/kmol)
N	number of CSTRs
$N(0, j)$	active site of type j produced by formation reaction
$N_d(j)$	spontaneously deactivated site of type j
$N_H(0, j)$	active site of type j produced by transfer to hydrogen
$N_i(r, j)$	live polymer of length r growing on site of type j with terminal monomer i
NS	number of types of active sites
P	pressure (Pa)
PDI	polydispersity index
$Q(r, j)$	dead polymer of length r produced at site of type j
R_A	rate of reaction for component A in the reactor (kmol/s)
R_k	instantaneous rate of reaction for monomer k (kmol/s)
R_p	production rate (kg/s)
R_v	volumetric flow rate of polymer from the reactor (m^3/s)
t	time (s)
T	temperature (K)
U_0	superficial gas velocity (m/s)
U_{mf}	minimum fluidization velocity (m/s)
V	reactor volume (m^3)
V_p	volume of polymer inside the reactor (m^3)
X	conversion
$X(n, j)$	nth moment of dead polymer produced at site of type j
$Y(n, j)$	nth moment of live polymer produced at site of type j
z	height above the distributor (m)

Greek letters

δ	volume fraction of bubbles in the bed
ε_b	void fraction of bubble
ε_e	void fraction of emulsion
ε_g	average void fraction of the bed
ε_{mf}	void fraction of the bed at minimum fluidization
τ_i	residence time of gas in the ith reactor (s)

related to its composition and the method of preparation. Therefore, unlike most of the ordinary catalyzed chemical reaction, the catalyst activity in polymerization process, and consequently the overall reaction rate, would be different from one operating mode to another. In case of low to moderate activity of the catalyst, heat transfer and diffusion resistances do not play an important role at the particle level in the gas-phase polyethylene reactors. In the limiting case, where either bubbles are small or interphase mass and energy transfer rates are high and catalyst is at low to moderate activity, intraparticle temperature and concentration gradients are negligible [10]. In this case, LLDPE production fluidized bed reactors could be modeled as a CSTR proposed by McAuley et al. [4]. However, as discussed above, such reactor may not be considered as a single CSTR. In the present work a tanks-in-series model is employed to model the fluidized bed reactor of LLDPE production in order to obtain a better understanding of the reactor performance.

2. Reactor modeling

A simplified flow diagram of gas-phase LLDPE production process is shown in Fig. 1. In this reactor, reactants (monomers and hydrogen) and inert gas (e.g., nitrogen) are

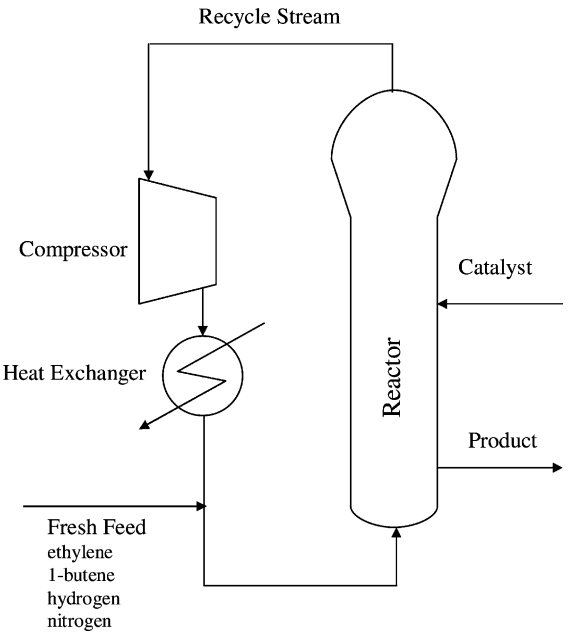

Fig. 1. Industrial fluidized bed polyethylene reactor.

fed into the bottom of the reactor through a distributor. The distributor maintains the fluidization and supplies the reactants for growing polymer particles. The catalyst is charged continuously into the bed and the polymer product is withdrawn from the reactor at a rate such that the bed height is held constant. Unreacted gases together with fine particles exit from the top of the bed through a curved disengaging zone at the upper part of the reactor. Settling of solid particles is facilitated in this section. The gas then enters a cyclone in order to separate the remainder particles and is combined with fresh feed stream after heat removal in the heat exchanger and then recycled to the base of the reactor.

In order to model the gas-phase LLDPE production fluidized bed reactor and develop the required non-ideal flow pattern, the bed is divided into several CSTRs in series, as shown in Fig. 2. Assumptions made in the present work for modeling such a reactor are as follows:

1. Materials in the reactor flow as a pseudo-homogeneous phase and average hydrodynamic properties of existing phases (bubble and emulsion) is used for describing the hydrodynamic characteristics of the bed.
2. The emulsion phase does not remain at minimum fluidization condition beyond the minimum fluidization velocity of gas and the bubbles may contain solid particles. Under such conditions the dynamic two-phase flow structure, proposed by Cui et al. [11], is employed to estimate the bed hydrodynamics. Other researchers [2,4,6] have employed simple two-phase model, which considers the emulsion to be in the minimum fluidization condition and existence of particle-free bubbles in the fluidized bed. However, the dynamic two-phase flow structure employed in this study provides a more realistic understanding of the phenomena encountered in the bed.

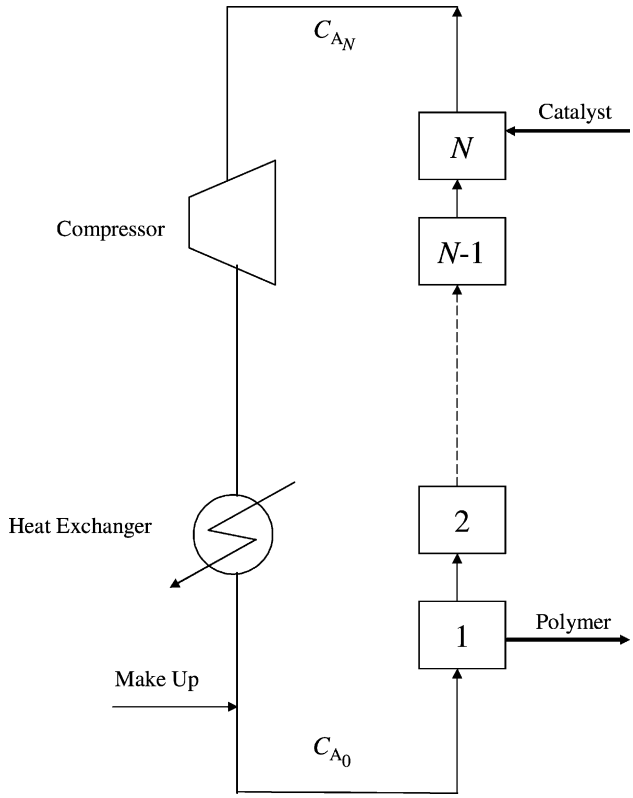

Fig. 2. Schematic diagram of the modeling structure.

3. There are negligible mass and heat transfer resistances between the solid polymer particles and emulsion gas (low to moderate catalyst activity). Also, mass and energy transfer resistances between the bubble and emulsion phases are neglected. Therefore, a pseudo-homogeneous single-phase model could be applied.
4. The reactor is in isothermal operation.
5. Radial concentration gradients in the reactor are negligible.
6. Elutriation of solids is neglected at the top of the bed.
7. Catalyst is fed continuously into the bed.
8. Constant mean particle size is assumed in the modeling.

Material balances for all CSTRs in series, as shown in Fig. 2, could be obtained easily [9]. For the *i*th reactor, this material balance is

$$C_{A_i} = C_{A_{i-1}} + \tau_i \frac{R_{A_i}}{\varepsilon_g V_i} = C_{A_{i-1}} + \frac{R_{A_i}}{\varepsilon_g A U_0} \quad (1)$$

In order to solve the model (Eq. (1)), one should specify the inlet concentration of each ingredient (monomers and hydrogen). These concentrations are known at the inlet of the reactor

$$C_{A_0} = C_{A_{in}} \quad (2)$$

In Eq. (1), the mean voidage of the bed, ε_g, and the overall reaction rate of each species, R_{A_i}, are two important quantities. Each of these quantities has to be determined using a suitable hydrodynamic and kinetic model.

2.1. Hydrodynamics

Up to now, most of the research works reported in the literature have employed the simple two-phase concepts for the gas-phase ethylene polymerization modeling (e.g., [4,6]). The simple two-phase hydrodynamic model assumes existence of particle-free bubbles in the fluidized bed while the emulsion remains at minimum fluidization conditions. However, the voidage of the emulsion phase may differ far from that at the minimum fluidization and also bubbles may contain different portions of solids [11]. Based on this concept, Cui et al. [11] proposed the dynamic two-phase structure for the fluidized bed hydrodynamics. Therefore, the assumption of the minimum fluidization condition for the emulsion phase in the polyethylene reactor (simple two-phase model) is not realistic. The difference between the simple two-phase (particle-free bubbles + emulsion at minimum fluidization) and the dynamic two-phase (particle concentration in emulsion and bubbles varies with gas velocity) have been investigated by Mostoufi et al. [12]. Although the reaction system in their work differs from that in the present work, it has been shown that assuming the simple two-phase structure of the fluidized beds would result in under-predicting the performance of the reactor. They concluded that such an oversimplification of the flow structure of gas and solids in the fluidized bed reactors could be quite misleading in the prediction of the performance of such reactors [12]. As a result, the dynamic two-phase flow structure of fluidized beds, proposed by Cui et al. [11], has been employed to calculate a better estimation of the average bed voidage. This model is applicable to both bubbling and turbulent regimes of fluidization. Since polyethylene produced in the reactor is Geldart B particle, the constants of Cui et al. [11] correlation were chosen accordingly. The correlations required to evaluate the average bed voidage from dynamic two-phase flow structure model are summarized in Table 1.

2.2. Kinetics

Catalytic polymerization of ethylene with α-olefin copolymers is rather complex and involves several reactions, both in series and parallel. This topic has been extensively reviewed by Dusseault and Hsu [13] and Xie et al. [1]. McAuley et al. [14] have proposed a comprehensive multi-site kinetic model for the copolymerization of olefins over heterogeneous Ziegler–Natta catalysts. The key elementary reactions, considered in this study, consist of the formation of active centers, insertion of monomers into the growing polymer chains, chain transfer reactions and catalyst deactivation. These elementary reactions are summarized in Table 2. Reactions with poisons are neglected in the present work since the contribution of the rate of such reactions is insignificant in the overall reaction scheme.

Table 1
Correlations required for evaluating the average bed voidage [11]

$$\varepsilon_g = (1-\delta)\varepsilon_e + \delta\varepsilon_b$$

$$\varepsilon_b = 1 - 0.146\exp\left(\frac{U_0 - U_{mf}}{4.439}\right)$$

$$\varepsilon_e = \varepsilon_{mf} + 0.2 - 0.059\exp\left(-\frac{U_0 - U_{mf}}{0.429}\right)$$

$$\delta = 0.534\left[1 - \exp\left(-\frac{U_0 - U_{mf}}{0.413}\right)\right]$$

Table 2
Elementary reactions of ethylene with α-olefins

Reactions	Description
$N(0,j) + M_i \overset{k_{i_i}(j)}{\rightarrow} N_i(1,j)$	Initiation reactions with monomers
$N_i(r,j) + M_k \overset{k_{p_{ik}}(j)}{\rightarrow} N_k(r+1,j)$	Propagation
$N_i(r,j) \overset{k_{fs_i}(j)}{\rightarrow} N_H(0,j) + Q(r,j)$	Spontaneous transfer
$N_i(r,j) + M_k \overset{k_{fm_{ik}}(j)}{\rightarrow} N_k(1,j) + Q(r,j)$	Transfer to monomer
$N_i(r,j) + H_2 \overset{k_{fh_i}(j)}{\rightarrow} N_H(0,j) + Q(r,j)$	Transfer to hydrogen
$N_i(r,j) + AlEt_3 \overset{k_{fr_i}(j)}{\rightarrow} N_1(1,j) + Q(r,j)$	Transfer to cocatalyst
$N_i(r,j) \overset{k_{ds}(j)}{\rightarrow} N_d(j) + Q(r,j)$	Deactivation reactions

The most common method of polymerization modeling is the method of moments. Application of the moments' method allows the prediction of the characteristics of the polymer, i.e., average molecular weight, polydispersity index, density and branching frequency as well as operating variables, i.e., consumption rate of the components (monomers and hydrogen) and the polymer production rate [14]. The corresponding moment equations are given in Table 3. McAuley et al. [14] proposed the following expression which assumes the significant consumption of monomers through the propagation reactions

$$R_k = \sum_{j}^{NS}\sum_{i}^{m}[M_k]Y(0,j)k_{p_{ik}}(j), \quad k = 1,2,\ldots \tag{3}$$

where NS is the number of types of active sites and m the number of types of monomers. According to this model, the cumulative rate of polymer production can be calculated from the following equation:

$$R_p = \sum_{k=1}^{m} mw_k\, R_k \tag{4}$$

These rates are evaluated after solving the moment equations by the method described by McAuley et al. [14].

3. Results and discussion

In order to demonstrate the predictive capabilities of the proposed model, simulations were carried out at the

Table 3
Moment equations used for polymer properties estimation and reaction rate calculations

$$\frac{dY(0,j)}{dt} = [M_T]\{k_{i_T}(j)N(0,j) + k_{h_T}(j)N_H(0,j)\} + k_{h_r}(j)N_H(0,j)[AlEt_3] - Y(0,j)\left\{k_{fh_T}(j)[H_2] + k_{fs_T}(j) + k_{ds}(j) + \frac{R_v}{V_p}\right\}$$

$$\frac{dY(1,j)}{dt} = [M_T]\{k_{i_T}(j)N(0,j) + k_{h_T}(j)N_H(0,j)\} + k_{h_r}(j)N_H(0,j)[AlEt_3] + [M_T]k_{pTT}(j)Y(0,j) + \{Y(0,j) - Y(1,j)\}\{k_{fm_{TT}}(j)[M_T] + k_{fr_T}(j)[AlEt_3]\} - Y(1,j)\left\{k_{fh_T}(j)[H_2] + k_{fs_T}(j) + k_{ds}(j) + \frac{R_v}{V_p}\right\}$$

$$\frac{dY(2,j)}{dt} = [M_T]\{k_{i_T}(j)N(0,j) + k_{h_T}(j)N_H(0,j)\} + k_{h_r}(j)N_H(0,j)[AlEt_3] + M_T k_{pTT}(j)\{2Y(1,j) - Y(0,j)\} + \{Y(0,j) - Y(2,j)\}\{k_{fm_{TT}}(j)[M_T] + k_{fr_T}(j)[AlEt_3]\} - Y(2,j)\left\{k_{fh_T}(j)[H_2] + k_{fs_T}(j) + k_{ds}(j) + \frac{R_v}{V_p}\right\}$$

$$\frac{dX(n,j)}{dt} = \{Y(n,j) - N_T(1,j)\}\{k_{fm_{TT}}(j)[M_T] + k_{fr_T}(j)[AlEt_3]\} + \{Y(n,j) - N_T(1,j)\}\{k_{fh_T}(j)[H_2] + k_{fs_T}(j) + k_{ds}(j)\} - X(n,j)\frac{R_v}{V_p}, n = 0, 1, 2$$

operating conditions shown in Table 4. Such operating conditions are typical of industrial polyethylene reactors for the grades indicated in this table. A comparison between the results of the model presented in this work with the actual plant data is made in Fig. 3 in terms of the melt flow index (MFI) of the produced polymer. As it could be seen in this parity plot, there is a good agreement between the calculated and measured MFI. The relation between the MFI and the molecular weight of polyethylene is given by the following equation:

$$\text{MFI} = 3.346 \times 10^{17} \bar{M}_w^{-3.472} \quad (5)$$

This equation is of the type proposed by McAuley et al. [14] with its constants being modified to fit the actual data presented in this work. The number of CSTRs given in Table 4 is chosen such that the reactor outlet fit the actual values.

The model developed in this work is able to predict the behavior of the reactor as well as the properties of the produced polyethylene in this reactor. In the following, results of the simulation are given for BP LL0209 grade as example. These results may be detailed in the following sections.

3.1. Reactor behavior

This part of result provides the information about the reactor operation such as conversion of components (i.e., monomers and hydrogen) and polymer productivity of the reactor. These results are as follows:

(a) Conversions of monomers along the bed height are shown in Fig. 4. As expected, conversion of monomers increases as the gas moves up in the bed. Total conversion is about 1.8% for ethylene and 0.15% for 1-butene in each pass of the gas through the reactor.
(b) Production rate of the polymer is calculated from Eq. (4) over the residence time of polymer in the reactor. The change of polymer production rate with residence time of the polymer is illustrated in Fig. 5. It could be seen in this figure that the production rate is about 2 t/h in 1 h and reaches about 5 t/h in 4 h after the reactor startup.

3.2. Polymer properties

This part of result provides the properties of the produced polymer based on the kinetic model used in this work:

(a) The number average and weight average molecular weight of the polymer can be calculated by the method described by McAuley et al. [14]. These values are shown in Fig. 6. This figure illustrates that the number and weight average molecular weight of the polymer increase rapidly at the beginning of the polymerization period and reach a constant value at less than an hour.

Table 4
Operating conditions of simulation

Parameter	BP LL0209	BP LL0640	BP LL0220	BP LL0410
D_t (m)	5	5	5	5
H (m)	14	14	14	14
d_p (μm)	1145	1145	1000	1000
T (°C)	72	75	72	72
P (bar)	20	20	20	20
U_0 (m/s)	0.57	0.56	0.57	0.57
Ethylene concentration (%)	40	39	40	40
1-Butene concentration (%)	17	11	17	13
Hydrogen concentration (%)	9	19	12	10
Inert gas concentration (%)	34	31	31	37
Catalyst feed rate (g/s)	0.2	0.2	0.2	0.2
Number of CSTRs (–)	3	3	3	3

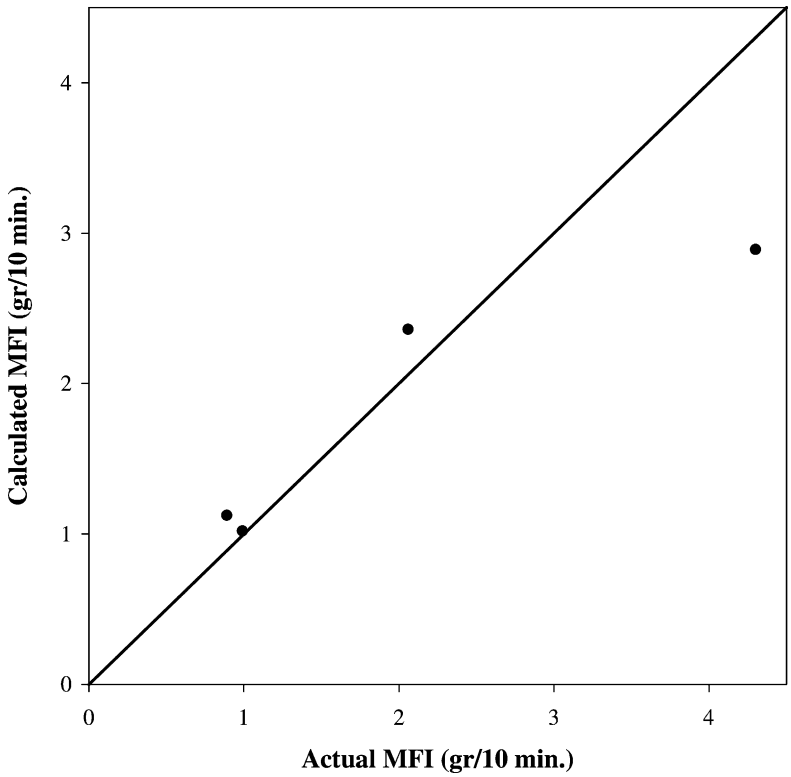

Fig. 3. Comparison between plant and calculated MFI.

The final value of weight average molecular weight, as shown in Fig. 6, is about 88 000.

(b) The molecular weight distribution of the produced polyethylene in outgoing flow is determined by the method applied by McAuley et al. [14]. Fig. 7 shows the molecular weight distributions of the polymer produced on each type of sites as well as the overall molecular weight distribution of the final product. The distribution shown

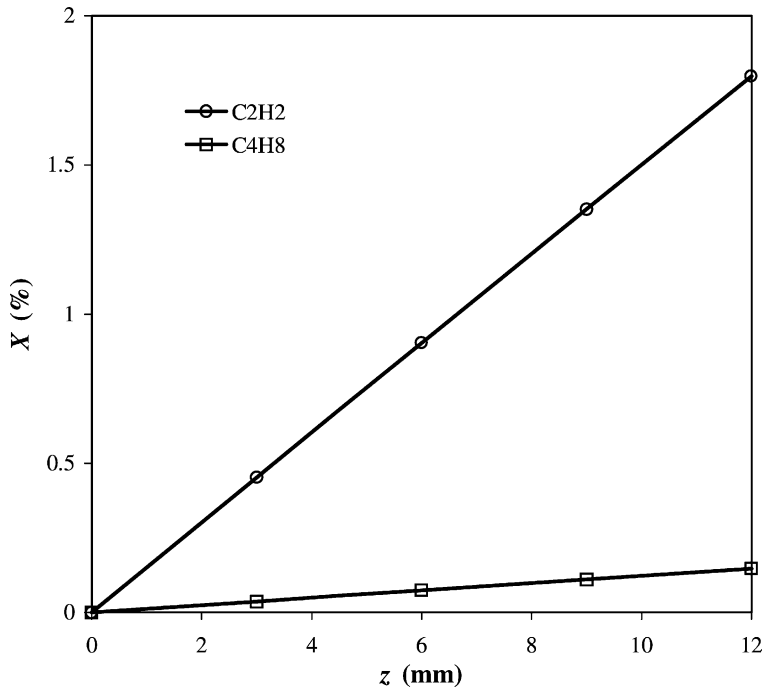

Fig. 4. Conversion of monomers along the bed height.

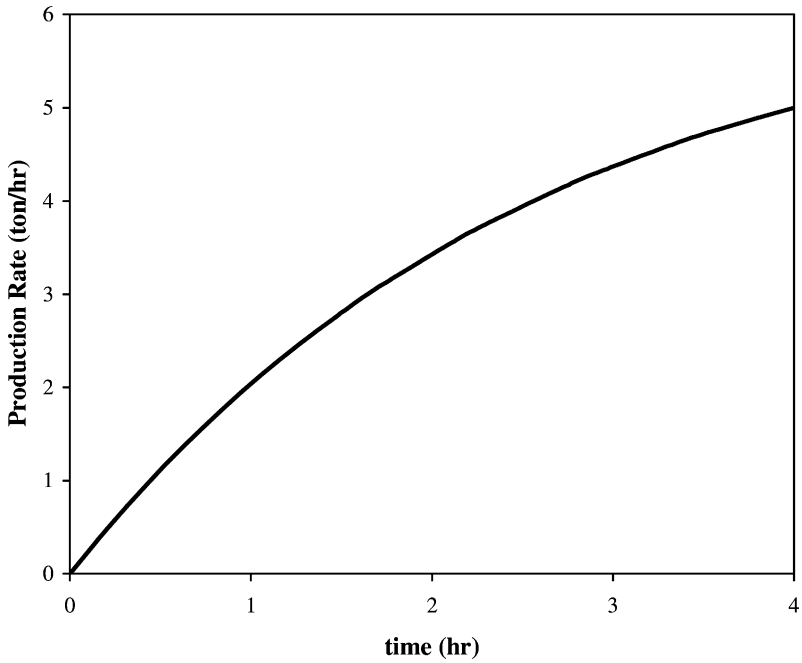

Fig. 5. Evolution of the production rate of the polymer over the residence time of the polymer in the reactor.

in Fig. 6 corresponds to a polyethylene sample which is taken at about an hour or more after startup of the reactor, when the reactor reaches the steady-state conditions.

(c) Polydispersity index of the polymer is defined as the ratio of weight average molecular weight to the number average molecular weight:

$$\mathrm{PDI} = \frac{\bar{M}_\mathrm{w}}{\bar{M}_\mathrm{n}} \tag{6}$$

This parameter has the same profile as average molecular weight during the course of polymerization. Evolution of this parameter with the residence time of the polymer in the reactor is illustrated in Fig. 8. The final value of the polydispersity index, in the conditions of this simulation, is stabilized close to 2.34, which shows that based on this calculation it is predicted a LLDPE will be produced with a narrow molecular weight

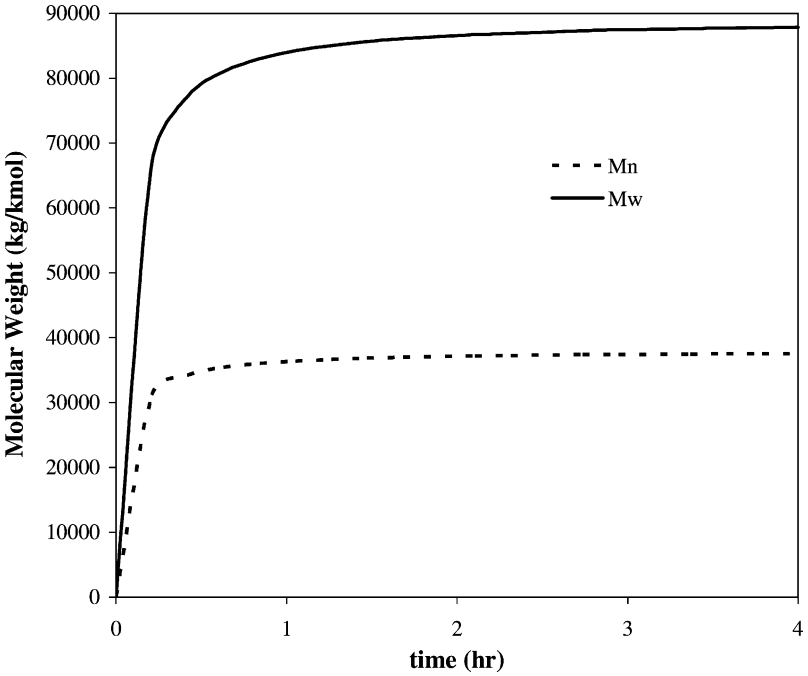

Fig. 6. Evolution of number and weight average molecular weights during the residence time of polymer in the reactor.

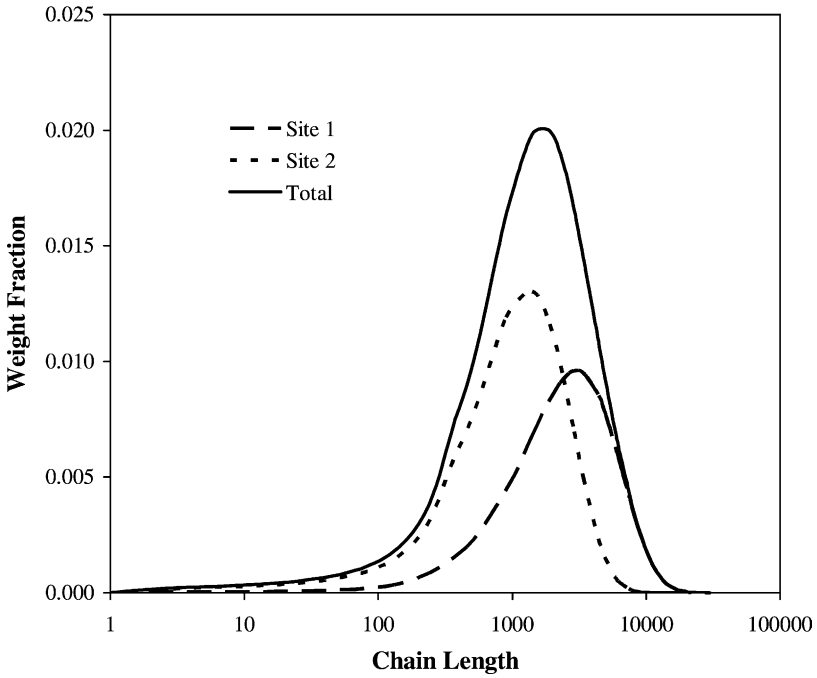

Fig. 7. Molecular weight distribution of the produced polyethylene.

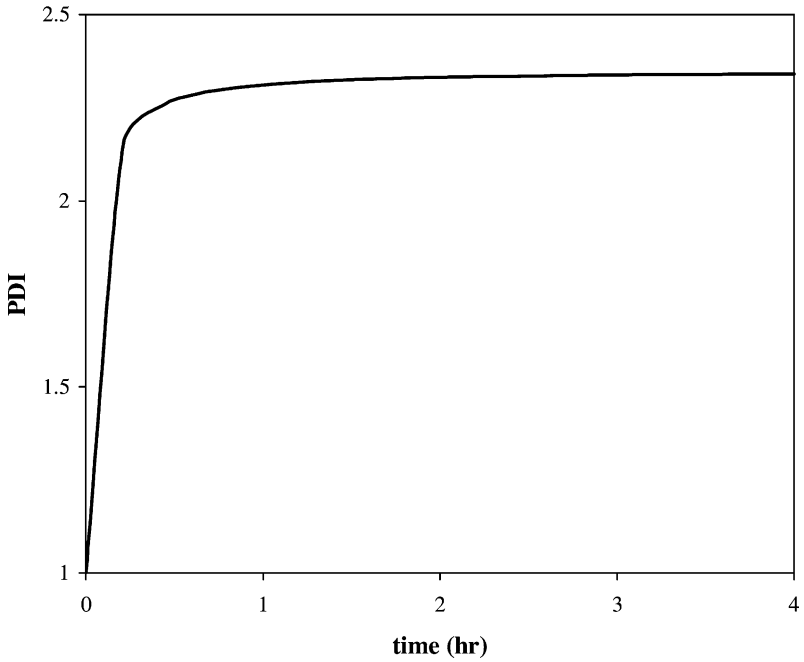

Fig. 8. Evolution of polydispersity index during the residence time of polymer in the reactor.

distribution. This is approved from the molecular weight distribution shown in Fig. 7.

4. Conclusions

A comprehensive model was developed for predicting the performance of industrial scale gas-phase LLDPE production reactors. The dynamic two-phase flow structure model was employed in this work which takes into account the presence of particles inside the bubbles as well as change of particle concentration in the emulsion phase with the superficial gas velocity in the reactor. Due to negligible heat and mass transfer resistances between the bubble and emulsion phases, a pseudo-homogeneous state was assumed throughout the fluidized bed. The tanks-in-series model was chosen

to describe the real flow pattern of the gas in the fluidized bed reactor of LLDPE production. This model is capable of predicting essential reactor parameters such as conversion and polymer productivity of the reactor. Moreover, the kinetic model used in this work enabled the prediction of the properties of the produced polymer such as average molecular weight, polydispersity index and molecular weight distribution of polymer to be possible in an implicit manner. The model presented in this work was compared with the actual data in terms of MFI and the agreement between actual and calculated data was found to be satisfactory. It is possible to use this model as a predictive tool to study the effects of operating, kinetic and hydrodynamic parameters on the reactor performance as well as polymer properties.

Acknowledgements

The authors would like to thank Tabriz Petrochemical Complex for their help and valuable comments. The financial support of the University of Tehran (grant no. 613/3/687) is gratefully acknowledged.

References

[1] T. Xie, K.B. McAuley, J.C.C. Hsu, D.W. Bacon, Gas phase ethylene polymerization: preparation processes, polymer properties and reactor modelling, Ind. Eng. Chem. Res. 33 (1994) 449–479.
[2] K.Y. Choi, W.H. Ray, The dynamic behaviour of fluidized bed reactors for solid catalyzed gas phase olefin polymerization, Chem. Eng. Sci. 40 (1985) 2261–2279.
[3] R.A. Hutchinson, C.M. Chen, W.H. Ray, Polymerization of olefins through heterogeneous catalysis. X. Modelling of particle growth and morphology, J. Appl. Polym. Sci. 44 (1992) 1389–1414.
[4] K.B. McAuley, J.P. Talbot, T.J. Harris, A comparison of two-phase and well-mixed models for fluidized-bed polyethylene reactors, Chem. Eng. Sci. 49 (1994) 2035–2045.
[5] F.A.N. Fernandes, L.M.F. Lona, Fluidized-bed reactor and physical–chemical properties modeling for polyethylene production, Comput. Chem. Eng. 23 (1999) S803–S806.
[6] F.A.N. Fernandes, L.M.F. Lona, Heterogeneous modelling for fluidized-bed polymerization reactor, Chem. Eng. Sci. 56 (2001) 963–969.
[7] W.H. Ray, Modelling of addition polymerization processes-free radical, ionic, group transfer, and Ziegler–Natta kinetics, Can. J. Chem. Eng. 69 (1991) 626–629.
[8] S.Y. Wu, J. Baeyens, Segregation by size difference in gas fluidized beds, Powder Technol. 98 (1998) 139–150.
[9] O. Levenspiel, Chemical Reaction Engineering, 2nd ed., Wiley, New York, 1999.
[10] S. Floyd, K.Y. Choi, T.W. Taylor, W.H. Ray, Polymerization of olefins through heterogeneous catalysts. III. Polymer particle modelling with an analysis of intraparticle heat and mass transfer effects, J. Appl. Polym. Sci. 32 (1986) 2935–2960.
[11] H.P. Cui, N. Mostoufi, J. Chaouki, Characterization of dynamic gas–solid distribution in fluidized beds, Chem. Eng. J. 79 (2000) 135–143.
[12] N. Mostoufi, H. Cui, J. Chaouki, A comparison of two- and single-phase models for fluidized bed reactors, Ind. Eng. Chem. Res. 40 (2001) 5526–5532.
[13] J.J.A. Dusseault, C.C. Hsu, $MgCl_2$-supported Ziegler–Natta catalysts for olefin polymerization: basic structure, mechanism, and kinetic behavior, JMS—Rev. Macromol. Chem. Phys. C 33 (2) (1993) 103–145.
[14] K.B. McAuley, J.F. MacGregor, A.E. Hamielec, A kinetic model for industrial gas-phase ethylene copolymerization, AIChE J. 36 (1990) 837–850.